Materials Research. 2021; 24(suppl. 1): e20210456
DOI: https://doi.org/10.1590/1980-5373-MR-2021-0456

Molecular Organization of Functionalized Carbon Nanotube at the Water-Air Interface and in Solid Thin Film

Vinicius Jessé Rodrigues de Oliveira[a]*, *Edilene Assunção da Silva*[a], *Clarissa de Almeida Olivati*[a]

[a] *Universidade Estadual Paulista (UNESP), Faculdade de Ciências e Tecnologia, Departamento de Física, Laboratório de Optoeletrônica e Filmes Finos, Rua Roberto Simonsen, 305, 19060-900, Presidente Prudente, SP, Brasil.*

Received: September 09, 2021; Accepted: September 23, 2021

Carbon Nanotubes (CNTs) are materials of wide applicability, either due to their physical stability, rigidity of the structure and/or high electrical conductivity. These nanotubes can be manipulated using different techniques, as long as their idiosyncrasy and possible advantages of proper processing are known. One way to organize and manipulate this material is in the form of thin films, which despite the low solubility in organic solvents, when functionalized, the CNTs allow for satisfactory handling. In this work, we aimed to analyze the behavior of CNTs in an aqueous subphase, controlling the quality of the produced films. For that, it was observed the level of aggregation and rigidity of Langmuir films and carried out analyses of the monolayer reorganization and interaction of the mixture between CNTs and Stearic Acid. Quantitative estimations of the aforementioned features were done through an in-situ study that was performed using the Langmuir technique including analysis of isotherms, compressibility module, Gibbs interaction, and Brewster Angle Microscopy. In order to compare the monolayer after its removal from the Langmuir trough, UV-vis spectroscopy was carried out. The results showed that they form non-ideal mixtures, but they favor a better organized and less agglomerated film comparing to the pure CNT.

Keywords: *Thin Films, Langmuir, Monolayer, Carbon Nanotube.*

1. Introduction

Most of the carbon composite materials are considered organic and exhibit several shapes, structures, and simple or complex characteristics that can be improved as needed. Carbon Nanotubes (CNTs) consist of rolled layers of graphene that form cylindrical tubes (Figure 1a). Such structured carbon allotrope has electrical and mechanical properties that are extremely resistant to environmental degradation and physical stresses[1]. These materials, today known as carbon nanotubes were discovered in 1991 by Iijima[2], through a transmission electron microscope (TEM) that was used to visualize the structured carbon material produced by the so-called "arc discharge method"[2]. Some similar structures had already been produced, but no interpretation was provided until the publication of Iijima, in which he reported on the potential of the new structure for possible studies and innovations. Since then, innumerous technological applications have been suggested, from LEDs[3-5], transistors, and gas sensors[6] to ballistic vests.

CNTs are organic and conductive rigid materials, which can be explored through several techniques already disseminated for other known conductive materials. Despite being poorly soluble, CNTs can be altered or functionalized to interact better with other chemical groups, enabling its processing through thin film techniques, in-situ analysis, and electrical measurements or spectroscopic analysis. From that, the behavior of the material under tension, electrical or optical stimulus is obtained[7].

Thus, it is compelling to use a number of techniques to investigate the properties of carbon nanotubes, whether it is to characterize or apply them to rising technologies. Another important aspect is to obtain an organized carbon nanotube structure arising from fabricating good quality films, which can tune preferable CNTs characteristics[8]. Herein, we have employed the Langmuir technique, UV-Visible spectroscopy, Brewster angle microscopy (BAM), to examine the nanotubes in aqueous subphase and its Langmuir-Schaefer films.

2. Experimental Section

2.1. Materials

The materials used in this study were single-walled carbon nanotubes, functionalized with Octadecylamine and an estimated molar mass of 847.97 g mol^{-1} (Figure 1a); and the stearic acid with a mass of 284,5 g mol^{-1} (Figure 1b), both materials were acquired commercially from Sigma Aldrich. Ultrapure water was obtained from a Millipore® water purification system. As a solvent for these materials during sample preparation, chloroform purchased from Synth was used.

2.2. Experimental procedures

2.2.1. Thin films fabrication

The solutions containing carbon nanotubes (CNTs) were prepared in two flasks, one containing only the pure material

*e-mail: *vinijro@gmail.com*

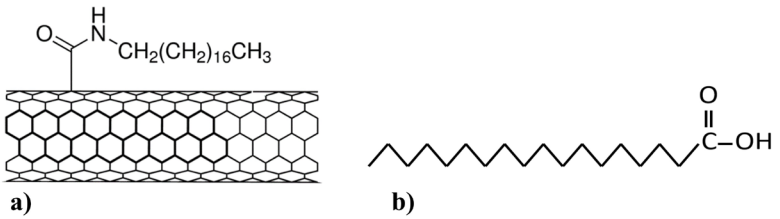

Figure 1. a) Single-Walled Carbon Nanotubes, functionalized Octadecylamine, b) Stearic Ácid.

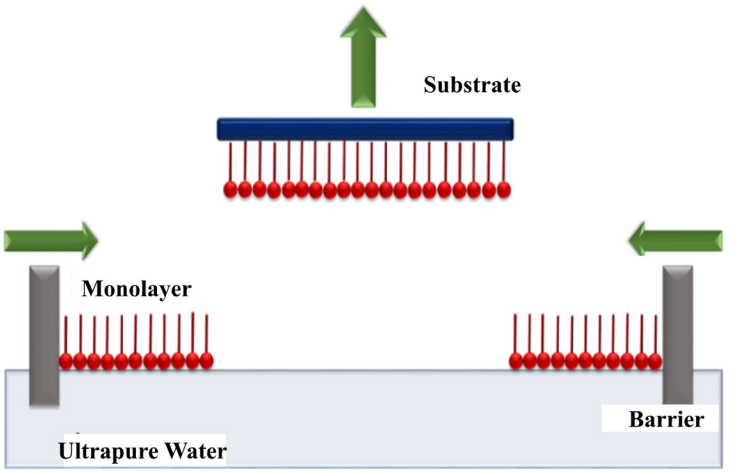

Figure 2. Schematic representation of the Langmuir Schaefer (LS) deposition.

and the other mixed with stearic acid (SA), both dissolved in chloroform. They were prepared in the following molar ratios (SA:CNT) of: 0:1 (pure CNT) and 1:1 (mmol) with total concentrations of 0.2 and 0.56 mg ml^{-1}, respectively. The solutions were placed in ultrasound for 8 hours due to the CNTs low solubility degree. The SA was used to help decrease the rigidity, and possibly to hinder the formation of aggregates in the aqueous subphase.

A Langmuir trough (model KSV 5000) was used to study and analyze molecules over the aqueous subphase. The subphase was filled with ultrapure water from a Millipore water purifier for retention particles with a 0.22 nm filter, producing water at 25 ºC with a resistivity of 18.2 MΩ.cm and pH = 6.4. The solution materials were dispersed drop-by-drop onto the water surface according to the information detailed in Table 1, and after spreading, it was allowed 15 minutes for the solvent evaporation and then the lateral barriers were started to compress the air-water interface.

During the compression of the monolayers, the surface pressures versus area per unit of the molecule, the so-called π-A isotherms, were analyzed. In this system, a Wilhelmy sensor monitors surface tension variations during the spreading and during the compression of the symmetrical lateral barriers of the trough, which compressed the material at a speed of 15 cm^2 min^{-1} [9,10].

After identifying, through π-A isotherms, the surface pressure value where the monolayers organization is in packed-like structure was then chosen to perform the transfer of the material onto the glass substrates. This transference served for the examination of the films properties when removed from the aqueous subphase. The deposition was made using the Langmuir Schaefer (LS) technique[11], in which the substrate positioned horizontally over the water subphase touches the water surface, and part of the monolayer adheres to the solid support, as shown in Figure 2.

Table 1. LS deposition parameters of CNTs and SA.

Proportion between SA and CNT (mmol)	0:1	1:1
Deposition Pressure (mN/m)	30	40
Spread Volume (μL)	1000	250
Layers	25	25

2.3. Thin films characterization

After the π-A isotherms acquisitions, the study on the transition phases of the material was deepened by performing an isotherm treatment for an assessment of the compressibility module (Cs^{-1}). During compression in the Langmuir trough, an in-situ analysis was performed using a Brewster Angle Microscope (BAM), in which the movement pattern and organization of the nanotubes during the formation of the rigid monolayer can be monitored. This analysis enabled the most assertive choice of the deposition parameter and, consequently, the transfer of the material to the glass substrate.

UV-Visible spectra of the LS films deposited onto the glass substrates were obtained using a Cary 100 UV-Vis spectrophotometer, making it possible to observe the main absorption bands of the films and determine an organization correlation between the material in the aqueous subphase and in its solid phase. This latter can be accomplished by analyzing the optical absorption band and the spectrum shift[10,12,13], these factors are known to provide some information concerning the film structure.

3. Results and Discussion

3.1. Langmuir isotherms (π-A)

In Figures 3 a) and b) we can see the π-A isotherms of pure and mixed CNTs with Stearic Acid. In both cases, the materials reached maximum pressure at similar values but presented a different behavior during the compression of the material. The material in its pure form showed a better organized (more packed) phase at a pressure of 30 mN m^{-1}, while the mixed CNTs just attained the condensed phase at 40 mN m^{-1}. With these respective values of surface pressures, the nanotubes, when pure and mixed with SA, had molecular areas of 38 and 32 $Å^2$, a fact that reveals the lesser formation of agglomerates and probable lower rigidity of the CNT monolayer after the incorporation of the amphiphilic molecule (SA).

Since the original average structure of carbon nanotubes should exhibit a large area if they are placed with the cylinder length parallel to the water surface. In this work, the nanotubes within the monolayers seem to be oriented perpendicularly or slightly inclined with respect to the surface. The nanotubes are poorly soluble, and exhibit a strong tendency to form large aggregates in aqueous media[14,15], corroborating the fact that they are rigid and can only be deposited via Langmuir-Schaefer (LS)[16]. The deposition parameters used during material processing in the Langmuir trough are in Table 1.

The graphs in Figure 3 show non-pronounced collapse pressure for the molecules since they do not actually "break"[17], but begin to approach due to the strong interaction that makes them aggregate. Both cases have collapse pressures around 60 mN m^{-1}, this shows the strong CNT-CNT interaction at the water-air interface, because, despite the mixture, the interaction between carbon nanotubes did not show any significant deviation from the collapse pressure[18,19].

When analyzing the π-A isotherms, Figure 3b) which contains a mixture between stearic acid and carbon nanotube, they show inflections in the curve, which would be a molecular reorganization occurring[20], this detail can be seen at pressures of 35 mN m^{-1}. Because of this possible transition, this pressure value was not chosen for the deposition since it is probably not in its condensed and stable phase[21].

An analysis was performed using the excess area average per molecule (SA)[18], according to Equation 1.

$$AE = A12 - \left(X1A1 + X2A2\right) \quad (1)$$

Which has as variables: A12 is the average molecular area in the two-component film, X1 and X2 are the two-component molar fractions, and A1 and A2 are the molecular areas of two unique components at the same chosen surface pressure[22-24].

The calculations performed in Equation 1 (additivity rule) were performed at a surface pressure of 40mN m^{-1}; analysis is done only for mixtures, with the objective of determining if we are working with an ideal phase mixture, that is, a completely homogeneous mixture, which presents all the thermodynamic phases of an ideal amphiphilic material when compressed in a Langmuir trough.. The respective calculation showed a value of 0.295 nm^2 for the mixture between CNTs and SA in 1: 1 mmol.

The aforementioned analysis uses the Gibbs free energy methods for mixtures, in which it considers the energy gain related to the joining of components to a system. As already calculated, the value of 0.295nm^2 is not null, meaning that the two materials aren't a perfect mixture[25,26]. The fact that the value is positive indicates a thermodynamically unstable process, that is, the binding energy between the components of the mixture does not present considerable binding forces between them, this compared to a pure solution[22,27,28].

Due to the low interaction force observed between these materials, even the ideal amphiphilic molecule aiding in the more homogeneous spacing of the CNTs did not make possible the deposition by the LB technique, which requires a more flexible monolayer, reason why it was essential

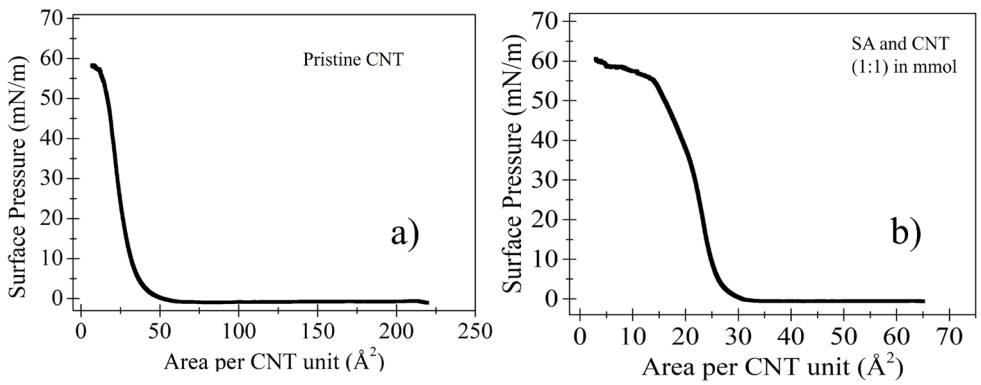

Figure 3. Isotherms (π-A) of (a) CNTs Pure and (b) CNTs with SA on ultrapure water subphase at room temperature (23 °C).

the use of the LS technique[19]. We can notice the presence of the SA causing the isotherm to deviate at a pressure of 35 mN m-1 (Figure 3b), which we can attribute to a molecular accommodation between the CNTs during the compression in the Langmuir trough[28].

A more detailed analysis of the molecular rearrangement that occurred during the compression of the material in the isotherm curves (π-A), can be analyzed with the modulus of compressibility curves (Cs^{-1})

3.2. Cs^{-1} vs A curves

The compressibilities of the monolayers were analyzed with the idea of understanding the details of the transition from expanded-liquid to the condensed-liquid phase. This phase transition is marked by an abrupt decrease in the area recorded during the compression isotherm of a material[28]. As a reference for an ideal compression module, we can use the pristine Stearic Acid curve as an amphiphilic material in a Langmuir trough as observed in the literature.

Figure 4a and b display the graphs of isotherms when analyzed by the compressibility modulus (Cs^{-1}) *versus* the area of the molecule, since this variable comes from a derivative it maximizes the details of the curves that are not perceptible in the isotherms.

$$Cs^{-1} = -A\left(\frac{d}{dA}\right)_T \quad (2)$$

Compressibility modulus equation (Cs^{-1} vs Area)

A represents the area per molecule, π is the surface pressure, and **Cs^{-1}** has a surface pressure unit (mN m^{-1}). The Cs^{-1} curves can be plotted as a function of surface pressure or area per unit of the CNT, allowing to estimate the transition phases of the materials when compressed[17,19,24].

The phase changes can be perceived when the graph stops oscillating around zero pressure, it is at these moments, that we can point out phase transition as it is more evident in Figure 4b), between pressures of 15 and 30 mN m^{-1}, pressures with more evident transitions. These transitions are followed by a reorganization of the mixture, where the peaks represent the maximum compressibility of that phase. We can notice that the pure CNTs did not have a peak higher than 125 mN m^{-1}, in the case of the mixed CNTs (Figure 4b) it reached a maximum above 250 mN m^{-1}, corresponding to the liquid-condensed phase[22,24,29].

3.3. Brewster angle microscopy

Using Brewster Angle Microscopy (BAM) measurements, it is possible to have a visual understanding of the material's behavior in the water-air subphase during compression, allowing the observation of domains and the formation of clusters. This fact can be seen in Figure 5, which depicts images obtained during the compression of pure CNT in the water subphase. We can observe a layer that covers the entire surface and the distribution of the material on it when reaching a surface pressure above 25mN m^{-1}. When observing the material in its mixed form with stearic acid (Figure 6), the formation of agglomerates tends to be less, where the dispersion of the CNTs is easier, which provides less rigidity for thin Langmuir films, and a better distribution of the material on the surface, reducing the large formation of clusters and agglomerates, in which the organization at 25 mN m^{-1} exhibits a surface well covered with material.

Figures 5 and 6 are images that possibly depict the thin film on the water, one of them is more agglomerated when pure, and the other is better dispersed in the subphase. This idea of better distribution is related to the ideal amphiphilic character of SA by establishing links of lesser intensity with CNTs, however allowing a greater dispersion of nanotubes. This idea of partial miscibility was observed through the quantitative analysis of Gibbs Free Energy for mixtures[27,30]. This value already presented shows that both mixed do not form a perfect mixture, but it allows a good dispersion of the nanotubes.

The pure material at its maximum compression shows a large agglomerate of material, apparently a rigid and entire surface like boards, while the mixture shows more homogeneous Langmuir films and apparently better distributed in the aqueous subphase, enabling a reorganization with the removal of each subsequent layer[30-33].

3.4. UV-Vis spectroscopy data

The level of organization of the materials, whether in solid or liquid phase, can be analyzed through optical absorption spectra, when submitted to a UV-Vis Cary 100 spectrophotometer for scanning the absorption spectrum. Figure 7a, b and c show the organization and linear growth obtained for the solutions and films of CNT and SA[34].

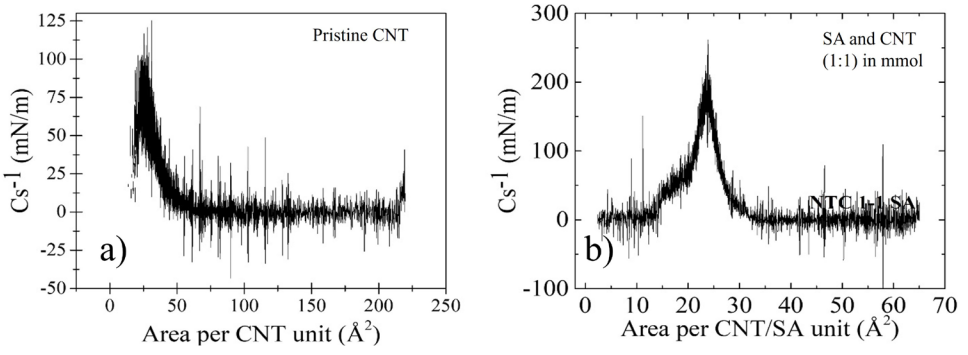

Figure 4. Area compressibility modulus (Cs-1 vs A) of the pristine and mixed CNT with stearic acid (SA): a) pristine CNTs and, b) 1:1 SA:CNTs.

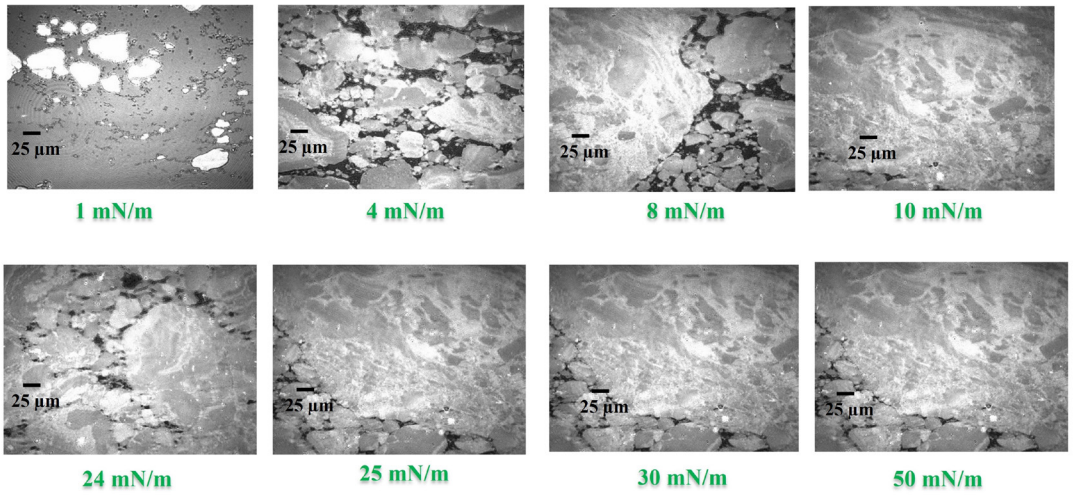

Figure 5. Image of compression of pure CNTs in aqueous subphase under Brewster's Angle Microscope (BAM).

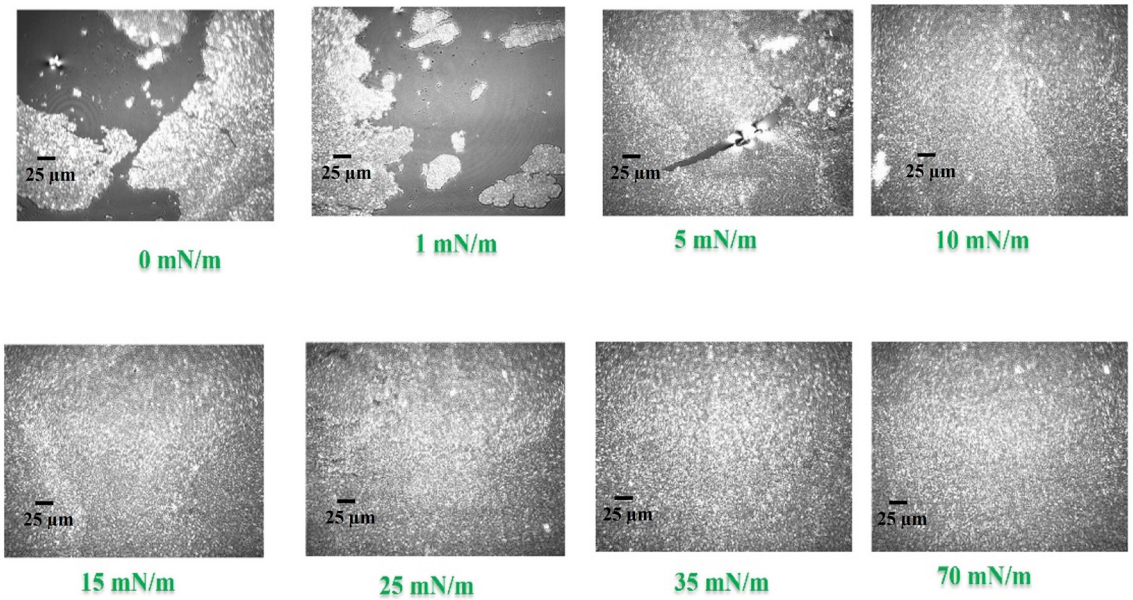

Figure 6. Image of SA and CNTs compression (1: 1) in aqueous subphase under Brewster's Angle Microscope (BAM).

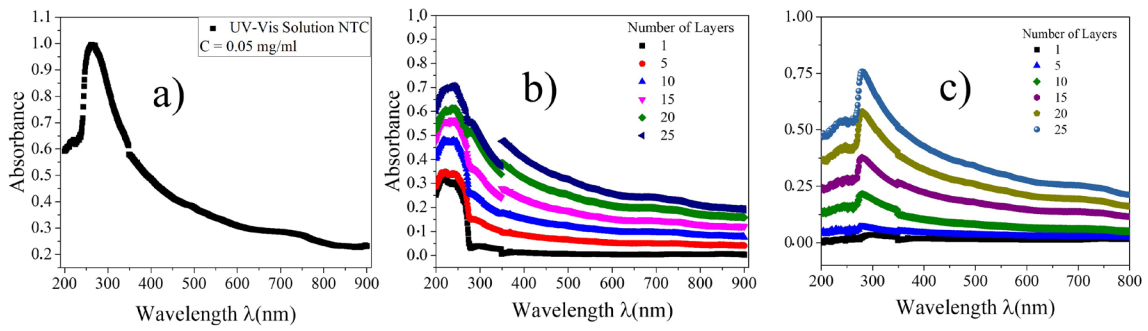

Figure 7. UV Vis da a) Pure CNTs solution, and thin film growth on the glass b) Pure CNTs and c) CNTs mixed with SA 1:1 (mmol).

The images obtained by UV-Vis confirm the better organization of the nanotubes in the form of films when mixed with SA. This can be affirmed by the spectra in Figure 7b and c where we can observe a redshift from a wavelength from 279 to 351 nm for the mixed monolayers (CNT and SA) deposited on the glass when compared to the pure CNT. This indicates a more organized and homogeneous film under the conditions of the mixture between the materials, either in situ or after the Langmuir was transferred onto the substrate[35-37].

4. Conclusions

We could show that functionalized CNTs can be processed by the LS technique, although when spread solely this material form a rather rigid and clustery monolayer. Thus, with the introduction of an ideal amphiphilic material, the SA, the CNT could be better dispersed over the water subphase. The rigidity and conformation of the films can be ascertained by the analyses of the CNT-CNT or the CNT-SA interactions of the materials. These features were observed in-situ through the isotherms, compressibility module, and BAM images, and subsequently with the UV-Visible spectroscopy of the LS films. From these evaluations, it was possible to notice the more flexible and organized profile of the mixed samples, evidencing the role of the SA molecule in decreasing the CNT-CNT interactions and, therefore, diminishing the aggregation so typical of these materials.

Acknowledgment

The authors are grateful for the financial support of the agencies CAPES, FAPESP, INEO/CNPq and CNPEM/LNNano, Grupo de Pesquisa "Laboratório de Materiais Nanoestruturados para Análises Ambientais e Biológicas" FCT UNESP, **"**This study was financed in part by the Coordenação de Aperfeiçoamento de Pessoal de Nível Superior - Brasil (CAPES) - Finance Code 001"

References

1. Maune H, Bockrath M. Elastomeric carbon nanotube circuits for local strain sensing. Appl Phys Lett. 2006;89:173131. http://dx.doi.org/10.1063/1.2358821.
2. Iijima S. Helical microtubules of graphitic carbon. Nature. 1991;354:56-8. http://dx.doi.org/10.1038/354056a0.
3. Bahena-garrido S, Shimoi N, Abe D, Hojo T, Tanaka Y, Tohji K. Plannar light source using a phosphor screen with single-walled carbon nanotubes as field emitters Plannar light source using a phosphor screen with single-walled carbon nanotubes as field emitters. Sci Instrum. 2014;85:104704-1-104704–6. http://dx.doi.org/10.1063/1.4895913.
4. Wang S, Zeng Q, Yang L, Zhang Z, Wang Z, Wang Z, et al. Light-emitting diodes with asymmetric contacts. Am Chem Soc. 2011;11:23-9. http://dx.doi.org/10.1021/nl101513z.
5. Gowri sankar PA, Udhayakumar K. A novel carbon nanotube field effect transistor based arithmetic computing circuit for low-power analog signal processing application. Procedia Technol. 2014;12:154-62. http://dx.doi.org/10.1016/j.protcy.2013.12.469.
6. Zaporotskova IV, Boroznina NP, Parkhomenko N, Kozhitov LV. Carbon nanotubes: sensor properties. A review. Mod Electron Mater J. 2016;2:95-105. http://dx.doi.org/10.1016/j.moem.2017.02.002.
7. Kumawat RL, Pathak B. Functionalized carbon nanotube electrodes for controlled DNA sequencing. Nanoscale Adv. 2020;2:4041-50. http://dx.doi.org/10.1039/D0NA00241K.
8. Kim Y, Minami N, Zhu W, Kazaoui S, Azumi R, Matsumoto M. Langmuir-Blodgett films of single-wall carbon nanotubes: layer-by-layer deposition and in-plane orientation of tubes. Jpn J Appl Phys. 2003;42:7629-34. http://dx.doi.org/10.1143/jjap.42.7629.
9. Citolino LVL, Braunger ML, Oliveira VJR, Olivati CA. Study of the nanostructure effect on polyalkylthiophene derivatives films using impedance spectroscopy. Mater Res. 2017;20(4):874-81. http://dx.doi.org/10.1590/1980-5373-MR-2016-0670.
10. Sakai A, Péres LO, Caseli L. Langmuir and Langmuir-Blodgett films of Cl-PPV mixed with stearic acid : implication of the morphology on the surface and spectroscopy properties. Colloid Polym Sci. 2015;293:883-90. http://dx.doi.org/10.1007/s00396-014-3477-4.
11. Braunger ML, Alessio P, Furini LN, Constantino CJL, Olivati CA, Influence of the supramolecular arrangement in the electrical conductivity of poly(thiophene) thin films. J Nanosci Nanotechnol. 2017;17:460-6. http://dx.doi.org/10.1166/jnn.2017.12667.
12. Seok J, Shin TJ, Park S, Cho C, Lee JY, Ryu DY, et al. Efficient organic photovoltaics utilizing nanoscale heterojunctions in sequentially deposited polymer/fullerene bilayer. Sci Rep. 2015;5:1-9. http://dx.doi.org/10.1038/srep08373.
13. Santos FH, Bühler AJ, Bagio N Fo, Zambra DAB. A importância da determinação do espectro da radiação local para um correto dimensionamento de conversão. Av En Energías Renov y Medio Ambient. 2015;19:11.42-11-54.
14. Silva IR, Barreto PLM, Bellettini IC. Study of aqueous dispersions of carbon nanotubes using different surfactants. Quim Nov. 2013;36(1):5-9.
15. Ji L, Lin Z, Li Y, Li S, Liang Y, Toprakci O, et al. Formation and characterization of core-sheath nano fi bers through electrospinning and surface-initiated polymerization. Polymer (Guildf). 2010;51:4368-74. http://dx.doi.org/10.1016/j.polymer.2010.07.042.
16. Gengler RYN, Veligura A, Enotiadis A, Diamanti EK, Gournis D, Józsa C, et al. Large-yield preparation of high-electronic-quality graphene by a Langmuir–Schaefer approach. Nano Micro Small. 2010;6:35-9. http://dx.doi.org/10.1002/smll.200901120.
17. Roberts G, editor. Langmuir-Blodgett films. USA: Springer; 1990.
18. Solletti JM. Characterization of mixed miscible and nonmiscible phospholipid Langmuir–Blodgett films by atomic force microscopy. J Vac Sci Technol B: Microelectron Nanom Struct Process. 1996;14(2):1492. http://dx.doi.org/10.1116/1.589125.
19 Petty MC. Langmuir-Blodgett films: an introduction. Cambridge: Cambridge University Press; 1996.
20. Belegrinou S, Dorn J, Kreiter M, Kita-tokarczyk K, Sinner E, Meier W. Biomimetic supported membranes from amphiphilic block copolymers. Soft Matter. 2010;6:179-86. http://dx.doi.org/10.1039/b917318h.
21. Horacek H. Gaskets with expandable graphite treated with nitric, sulphuric, phosphoric acids and ferric chloride, open access. Libr J. 2015;2:e1297. http://dx.doi.org/10.4236/oalib.1101297.
22. Jessé V, De Oliveira R, Assunção E, Braunger ML, Awada H, De Santana H, et al. Molecular organization relationship of low-bandgap polymers at the air-water interface and in solid films. J Mol Liq. 2018;268:114-21. http://dx.doi.org/10.1016/j.molliq.2018.07.018.
23. Rosen MJ, Zhou Q. Surfactant-surfactant interactions in mixed micelle formation. Langmuir. 2001;17(12):3532-7. http://dx.doi.org/10.1021/la001197b.
24. Dennison SR, Harris F, Phoenix DA. A Langmuir approach on monolayer interactions to investigate surface active peptides. Protein Pept Lett. 2010;17(11):1363-75. http://dx.doi.org/10.2174/092986651100901136 3.

25. Modlińska A, Bauman D. The Langmuir-Blodgett technique as a tool for homeotropic alignment of fluorinated liquid crystals mixed with arachidic acid. Int J Mol Sci. 2011;12:4923-45. http://dx.doi.org/10.3390/ijms12084923.
26. Gaines GL Jr. Thermodynamic relationships for mixed insoluble monolayers. J Colloid Interface Sci. 1966;21(3):315-9.
27. Nakahara H, Hirano C, Fujita I, Shibata O. Interfacial properties in langmuir monolayers and LB films of DPPC with partially fluorinated alcohol (F8H7OH). J Oleo Sci. 2013;62:1017-27.
28. Yu Z, Jin J, Cao Y. Characterization of the liquid-expanded to liquid-condensed phase transition of monolayers by means of compressibility. Langmuir. 2002;18:4530-1.
29. Haefele T, Kita-tokarczyk K, Meier W. Phase behavior of mixed langmuir monolayers from amphiphilic block copolymers and an antimicrobial peptide. Langmuir. 2006;22:1164-72. http://dx.doi.org/10.1021/la0524216.
30. Nabok A. Organic and inorganic nanostructures. USA: Artech House Publishers; 2005.
31. Callister WD Jr. Materials science and engineering - an introduction. Rio de Janeiro: LTC; 2007.
32. Lheveder C, Hénon S, Mercier R, Tissot G, Fournet P. A new Brewster angle microscope a new Brewster angle microscope. Rev Sci Instrum. 1998;1446:1-6. http://dx.doi.org/10.1063/1.1148779.
33. Abe A. Polymer Analysis/Polymer Theory (Advances in Polymer Science (182). USA: Springer; 2005.
34. Belarusian State University, Department of Energy Physics, TEMPUS program of the European Union, Project 530379-TEMPUS-1-2012-1-LVTEMPUS-JPCR "Energy". Study of semiconductors by UV-Vis spectroscopy. Guidelines for laboratory work. Europe: European Union; 2012. p. 1-15. Available from: http://www.physics.bsu.by/sites/default/files/files/departments/Energy/TEMPUS/CMM_lab/Characterization%20of%20modern%20materials%20-%20Study%20of%20semiconductors%20by%20UV-Vis%20spectroscopy%20-%20TEMPUS%20%28english%20version%29.pdf
35. Niu JZ, Cheng G, Li Z, Wang H, Lou S, Du Z, et al. Poly (3-dodecylthiophene) Langmuir-Blodgett films: preparation and characterization. Colloids Surf A Physicochem Eng Asp. 2008;330:62-6. http://dx.doi.org/10.1016/j.colsurfa.2008.07.041.
36. Falke S, Eravuchira P, Materny A, Lienau C. Raman spectroscopic identification of fullerene inclusions in polymer/fullerene blends. J Raman Spectrosc. 2011;42:1897-900. http://dx.doi.org/10.1002/jrs.2966.
37. Rhodes EWT, Adibi EBA, Asakura T, Kamiya T, Krausz F, Monemar B, et al. Springer Series in Optical Sciences. USA: Springer; 2009.